Modeling PVTX Diagrams: Application to Various Blends Based on Unsaturated Polyester—Influence of Thermoplastic Additive, Fillers, and Reinforcements

N. Boyard,[1] M. Vayer,[1] C. Sinturel,[1] R. Erre,[1] D. Delaunay[2]

[1]*Centre de Recherche sur la Matière Divisée, 1 B rue de la Férollerie, 45071 Orleans Cedex 02, France*
[2]*Ecole Polytechnique de l'Université de Nantes-Laboratoire de Thermocinétique, UMR CNRS 6607 Rue Christian Pauc, 44306 Nantes, France*

Received 30 May 2003; accepted 22 January 2004

ABSTRACT: The model previously proposed to predict the volume change of filled blends was extended to unsaturated polyester/styrene blends without or with thermoplastic additive and to blends with fillers and/or fibers. This model was based on experimental results from Pressure Volume Temperature X (PVTX) setup where temperature, conversion degree, and volume at a controlled pressure were monitored simultaneously. Predictions obtained from the model were compared to experimental results and were in good agreement. This model took into account thermal expansion, polymerization shrinkage, and shrinkage compensation via porosity formation. These phenomena were deconvoluted from the experimental curve and separately quantified. It was shown that shrinkage and its compensation induced a volume variation exhibiting a linear dependence with conversion degree. The influences of low-profile additive content, pressure, fillers, and fiber presence on shrinkage control were highlighted. © 2004 Wiley Periodicals, Inc. J Appl Polym Sci 92: 2976–2988, 2004

Key words: crosslinking; modeling; thermostats; voids; kinetics

INTRODUCTION

The macroscopic volume variation occurring during the processing of unsaturated polyesters (UP) are of fundamental and economic importance because it determines surface aspect, warpage, and dimension of the final product.[1] As demonstrated by numerous experimental studies,[2–8] the global volume variation under curing is a complex function resulting from the convolution of elementary phenomena that can be qualitatively described as follows: thermal variation (expansion and contraction), resulting from the dynamic conditions of cure; polymerization shrinkage, related to the reduction of steric hindrance of the macromolecular system with conversion; pores formation, resulting from the local stress relaxation that contributes to a macroscopic shrinkage compensation; vitrification, observed if the glass transition temperature reaches the temperature of the curing reaction[9] (in the case of dynamic curing, a succession of vitrification/devitrification can be observed).

The development of a model integrating these elementary phenomena (thermal dilatation, shrinkage, shrinkage compensation, and state change during the heating) is a challenging task. It would lead to a realistic simulation of the volume variation, helping for process optimization. Few models[10–12] are available in the literature and moreover do not consider all of the basic items previously exposed. These authors have included both thermal effects and polymerization shrinkage effect but the step of shrinkage compensation has never been mentioned.

In a previous article, a model for dynamical curing was proposed.[13] It is based on experimental results carried out on a filled ternary blend with equipment built at the laboratory, where volume, temperature, and heat flux were measured simultaneously at a given pressure.

This model takes into account thermal expansion, polymerization shrinkage, and associated shrinkage compensation. The main hypothesis is the proportionality between the shrinkage variation rate and the reaction rate. This model shows that shrinkage compensation for filled ternary blend does not start at the same time as shrinkage but when conversion degree is higher than 30%.

The aim of this work was to confirm the previously mentioned hypothesis by studying a blend without any shrinkage compensation, to apply, and to extend the model to binary, ternary blends, and to the corresponding filled blends. For this purpose, shrinkage and its compensation have to be deconvoluted and separately quantified. The influences of fillers, low-

Correspondence to: M. Vayer (marylene.vayer@ univ-orleans.fr).

Journal of Applied Polymer Science, Vol. 92, 2976–2988 (2004)

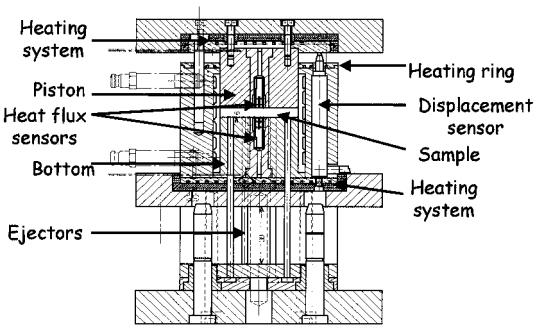

Figure 1 Scheme of PVTX setup.

profile additive content, and pressure were also studied.

EXPERIMENTAL

Samples description

The following binary blend (BB) samples were prepared on the basis of a UP prepolymer and styrene (ST) as curing agent. The UP prepolymer (M_n = 2700 g mol^{-1}) was Palapreg P18-03 from DSM Composite Resins (Germany) made from a 1 : 0.7 : 0.3 mixture of maleic anhydride, propylene glycol, and neopentyl glycol ST was provided by Cray-Valley (France). The ST double-bond to UP double-bond ratio was set at a value of 2.0. Tertiobutyl-ethyl 2-perhexanoate from Peroxide-Chemie GmbH (Germany) is added as polymerization initiator (1 wt %).

The following ternary blends (TB) samples were prepared. A thermoplastic additive as low-profile additive (LPA) was added to the binary blend as previously described. The LPA was a noncommercial saturated polyester made and provided by Cray Valley (France). The LPA (M_n = 2690 g mol^{-1}) was saturated polyester based on adipic acid and propylene glycol. The LPA contents based on pure solid saturated polyester was 5, 15, and 25 wt % of the total weight of the UP/ST/LPA ternary blend.

The following binary blend and fillers (BBF) samples were prepared: the BB previously described was completed with calcium carbonate ($CaCO_3$) fillers OMYA carb 80 OG from OMYA (France). This blend was composed of 36 wt % BB and 64 wt % $CaCO_3$.

The following ternary blend and filler (TBF) samples were prepared. They were composed of 24 wt % TB and 75 wt % $CaCO_3$. The LPA content in the TB was 13 wt %. Calcium stearate (1 wt %) CECAVON from CECA (Atofina, France) was also added as demolding agent.

The following non-commercial bulk molding compound (BMC) made and provided by Menzolit Company (France) was also studied to validate the proposed model for composite system. It was composed of 20.1 wt % TB containing 25 wt % LPA, 20 wt % of glass fibers, 58.9 wt % of fillers ($CaCO_3$), and 1 wt % calcium stearate.

Instrumentation and procedures

The device used for measurements is presented in Figure 1. It was previously described[13] in detail. Modifications, however, were performed to lower possible gradients of pressure and temperature. An additional heating resistance was introduced in the core of the mold. The sample, a 50-mm-diameter disk, is compressed between the mold bottom and a mobile piston moving inside the cylindrical lateral wall.

This mold was only usable for samples which were not likely to be liquefied during their thermal history. Material loss was thus avoided.

Blends added with fillers exhibit high viscosity and could be cured in this mold. Introduction of calcium stearate as demolding agent prevented the cured system from sticking on the mold.

Other samples such as binary and ternary blends were initially viscous but liquefy with the increase of temperature. This induced losses and demolding problems. To study these samples, a molding cavity made of elastomer was developed. This elastomer material was deformable but incompressible. This cavity comprised a base and a top welded together by a special adhesive. The walls of the cavity were 1 mm thick and the internal volume was 1.6 cm^3. The binary and ternary blends were introduced by means of a syringe. The cavity was placed in the mold. After molding, the sample was 6 mm thick. The filled thermoset blends (BBF, TBF, and BMC) before curing was adjusted (18 g) to mold a cylinder 5 mm thick.

The pressure in molding cavity was either 1.6, 4.8, or 8.0 MPa. The temperature cycle started at 40°C for 15 min. Temperature increased linearly to 160°C at 5 K/min and was maintained at 160°C for 15 min and then decreased to 40°C. A second identical cycle was performed to calibrate heat flux and to evaluate thermal expansion coefficient.

For filled thermoset blends, the applied pressure was sufficient to ensure a hydrostatic pressure within the sample. In addition, the fillers, which had good heat conductivity, ensured a good heat conduction inside the sample. Consequently, the temperature and conversion degree gradients in the sample under heating are limited, considering its small thickness and the moderate heating rate. It was verified by calculations.[12]

For binary or ternary blends molded into the elastomer cavity, the samples were less conductive and the elastomer cavity induced a thermal resistance. Consequently, there was a delay with the measurement of heat flow and a more significant temperature gradient probably exists in the sample. Moreover, be-

low a critical pressure, the contact between the piston, the bottom, and the sample was not good enough and the measurement of sample thickness was disturbed. The inferior limit value was shown to be 1.6 MPa.

The temperature data are processed following a procedure described in the previous article.[13] During the first cycle, the heat flux was due to exothermal polymerization reaction, sample heat capacity before, during, and after curing, and possibly heat losses of device. The heat flux during the second cycle was only due to cured blend heat capacity and experimental device heat losses. The heat flux generated by the crosslinking reaction was thus obtained by subtracting the heat flux of the second cycle to the one of the first cycle.

When the temperature increased, the mold, the sample, and the elastomer cavity exhibited volume variations and the displacement detector response combined these effects.

The thickness of the filled blend during the thermal cycle was obtained by subtracting the response of an aluminum standard (diameter = 50 mm, thickness = 5.07 mm) with known thermal expansion.

In the case of binary and ternary blends, we used as standard an aluminum cylinder with a diameter of 58.4 mm and a thickness of 6 mm introduced inside the elastomer cavity. As this elastomer can be considered as an incompressible fluid on a mechanical point of view, the subtraction of this response to the displacement recorded for elastomer cavity filled with ternary or binary blend only gave the blend thickness.

RESULTS AND DISCUSSION

Flux results, kinetics of reaction

During the copolymerization, an exothermic heat of reaction, which can be monitored, accompanied the conversion of the double bond to single bond. From the heat flux curves (dQ/dt in J m^{-2} s^{-1}) as a function of time t, the enthalpy of crosslinking (ΔH), the conversion degree (X), and the rate of cure (dX/dt) can be obtained as

$$\Delta H = \frac{Q_T}{e\mu p} \quad X = \frac{Q_t}{Q_T} \quad \frac{dX}{dt} = \frac{1}{Q_T}\left(\frac{dQ}{dt}\right)$$

where Q_T (J) is the total heat of reaction, e is the sample thickness (m), μ is the specific mass (kg m^{-3}) of the polymer blend, p is the relative amount of thermoset resin in the blend, and Q_t is the heat of reaction at a given time t.

As shown in Figure 2(a), the heat of reaction observed for the curing cycle became negligible as early as 130°C. Moreover, any residual exothermic heat flux was not observed in the second heating cycle. Previous experiments with a higher curing temperature (180°C) have confirmed that the samples were fully cured after the first cycle. Consequently, all the reactive styrene monomer and the C═C double bonds of unsaturated polyester were consumed at the end of the first cycle of curing.

Table I show ΔH for the various samples. Except for TBF, on the same UP/ST mass basis, no significant variation of the values was observed, indicating a rather similar degree of cure for all the samples. The higher value observed for TBF will be explained at the end of this section.

Examples of raw data concerning the flux as a function of temperature and of kinetics of reaction dX/dt as a function of temperature and conversion are presented in Figure 2(a–c), respectively. It was observed in Figure 2(b) that the rates of reaction exhibited rather similar shapes first with an induction period corresponding to a temperature range where the peroxides were stable and/or the radical formed was trapped in the media. The rate of reaction then increased because of the continuous increase of temperature, reached a maximum, and eventually decreased. To explain such a behavior, the concept of autoaccelerated reaction (Trommsdorff effect), which is based on the control of the kinetics of reaction by diffusion, have been already proposed by numerous authors.[14–16] It is generally admitted that termination reaction is first limited, leading to an increased concentration of radicals at the onset of the reaction, that explained the initial increase of the reaction rate. As the conversion degree increased, the mobility dropped and the propagation itself became diffusion limited (vitrification could here occur). Physical modifications of the system upon curing (structural inhomogeneities, phase separation) also played a significant role in the kinetics control. These phenomena, associated with continuous monomer depletion, then induced a global limitation of reaction rate.

Within this general scheme, however, one noticed different behaviors for the samples with and without fillers. The blends without fillers exhibited a longer induction period [Fig. 2(b)], suggesting that fillers acted as a catalyst for peroxide decomposition.[17–18] As a consequence, the copolymerization reaction began later for unfilled blends, but their reaction rates were higher for low conversion degree [Fig. 2(c)] because the temperature was higher when the polymerization started. The comparison of BB and TB curves did not show influence of LPA on reaction rate.

For the blends with fillers (BMC, TBF, BBF), the curves dX/dt as a function of time [Fig. 2(d)] presented a shoulder associated with an increased noise/signal ratio. This behavior was characteristic of successive vitrification/devitrification of the sample, indicating that the glass transition temperature of the system reached a value equal to the sample temperature.[9] The inverse method[19] we applied to determine the flux from temperature measurement was indeed not able to take into account this phenomenon, which

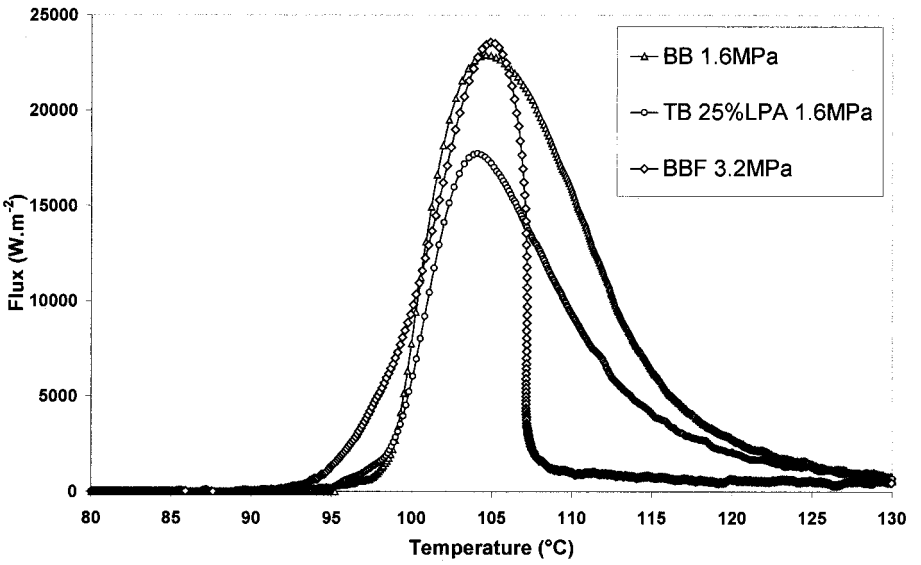

(a)

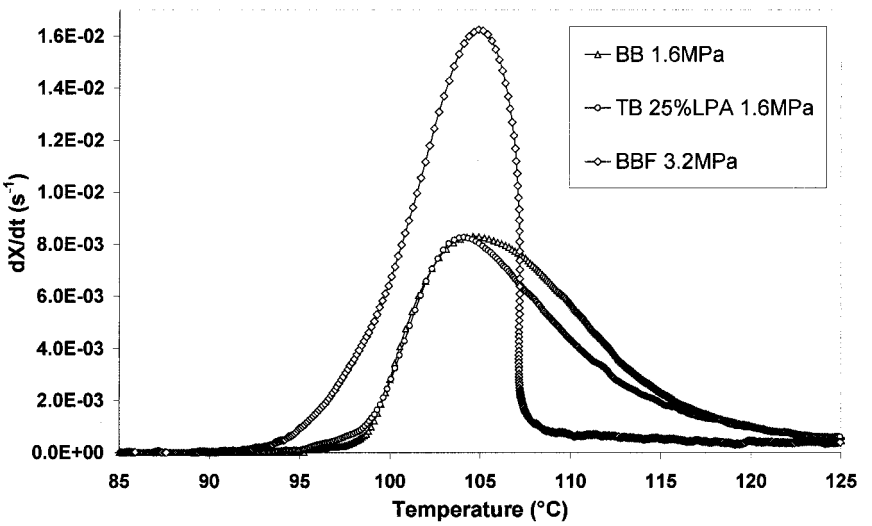

(b)

Figure 2 (a) Heat flux (dQ/dt) as a function of temperature. (b) Reaction rate (dX/dt) as a function of temperature. (c) Reaction rate (dX/dt) as a function of conversion degree (X). (d) Heat flux dQ/dt as a function of time for TBF at 1.6 MPa. The arrow indicates the critical point where a succession of vitrification/devitrification is encountered.

corresponded to a dramatic drop of the heat flux to zero value. The high value of ΔH measured for these blends especially for TBF was explained by the integration over the whole area under heat flux curve. This led to an overestimation of this ΔH.

Dilatometric results

Raw dilatometric curves

During the experiments, all the studied blends presented the same type of thickness evolution as a function of time (Fig. 3). As the temperature rose, the thickness first increased, reached a maximum, and decreased to a minimum before it increased again and eventually reached a plateau because of temperature stabilization.

These thickness variations were due to the superposition and the combination of thermal expansion, polymerization shrinkage, and volume expansion due to pore formation. The thickness $e(t)$ was thus the sum of the initial thickness e_0, the thickness variation due to the thermal expansion (Δe_T), and the contribution of cure phenomena (shrinkage and the associated compensation) to the thickness variation of the sample (Δe_{SC}). $e(t)$ can be expressed as [13]:

$$e(t) = e_0 + \Delta e_{SC} + \Delta e_T$$

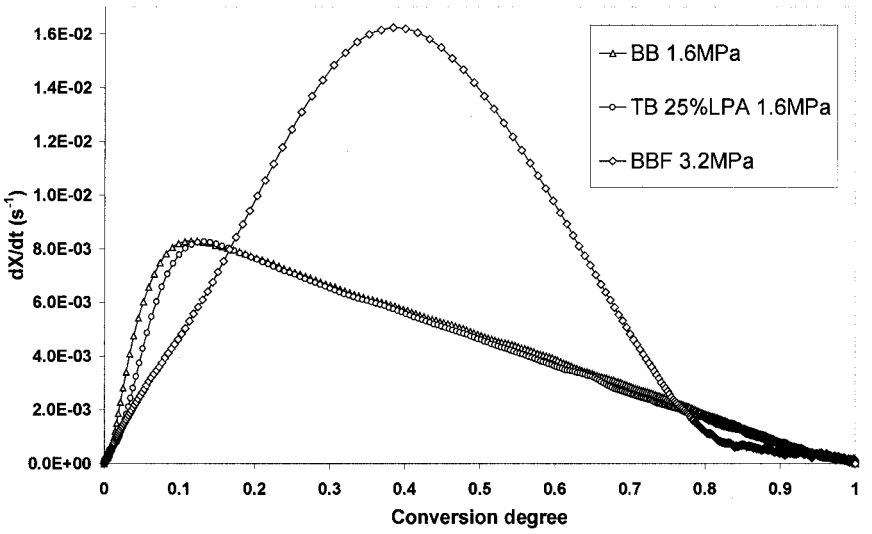

(c)

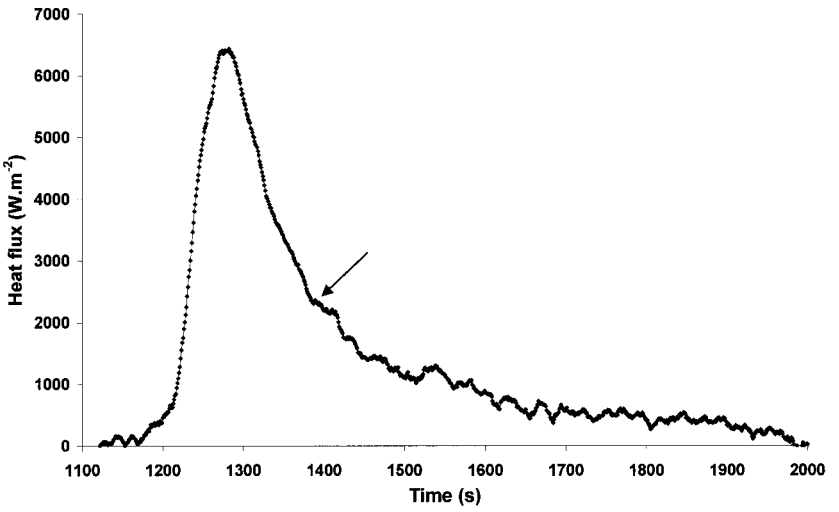

(d)

Figure 2 (*Continued from the previous page*)

Estimation of the thickness variation due to thermal expansion (δe_t)

To obtain thickness variation due to cure (Δe_{SC}), thermal expansion (Δe_T) had to be evaluated and subtracted from the experimental thickness. As demonstrated in a previous article,[13] the theoretical expression of the thermal expansion between T_0 and T is defined by

$$\Delta e_T = \int_{T_0}^{T} e(t)\alpha(X, T, P)\, dT \quad \text{with} \quad \alpha = \frac{1}{e}\left(\frac{\partial e}{\partial T}\right)_{P,X}$$

where α is the thermal expansion coefficient. This can be rewritten in a simpler way:

$$\Delta e_T = \int_{T_0}^{T} \left(\frac{\partial e}{\partial T}\right)_{P,X} dT$$

In practice, the thickness behavior was divided in three periods.

TABLE I
Total Enthalpies of Crosslinking

	(ΔH) (J g^{-1})	(ΔH) (J g^{-1}) on a total UPST mass basis
BB	424	424
TB (5% LPA)	404	425
TB (15% LPA)	369	434
TB (25% LPA)	314	418
TBF	122	602[a]
BBF	150	416
BMC	66	—

[a] Overestimated value due to a successive vitrification/devitrification phenomenon.

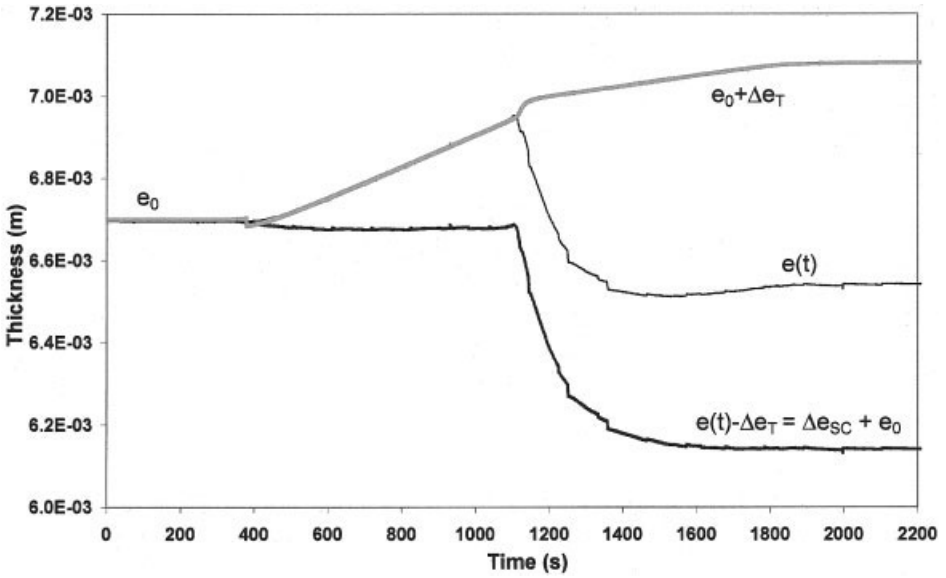

Figure 3 Experimental curve $e(t)$, e-Δe_T, $e_0 + \Delta e_T$ as a function of time (t) for BB at 1.6 MPa.

Between the initial temperature T_0 and the temperature T_i at which the reaction began, the thickness $e(T)$ was a quasi-linear function of the temperature T: $e(T) = k_0(T - T_0) + e_0$. This gave

$$\Delta e_T = k_0(T_i - T_0)$$

with

$$k_0 = \left(\frac{\partial e}{\partial T}\right)_{P,0} \quad \text{and} \quad \alpha_0 = \frac{k_0}{e_0}$$

characteristic of the uncured state (assuming here that the thickness variations are small compared to the thickness of the sample).

After curing, between the temperature at the end of the reaction (T_f) and the temperature at the end of the experiment (T_e), the thickness also evolved as a linear function of the temperature $e(T) = k_1(T - T_f) + e_1$:

$$\Delta e_T = k_1(T_e - T_f)$$

with

$$k_1 = \left(\frac{\partial e}{\partial T}\right)_{P,1} \quad \text{and} \quad \alpha_1 = \frac{k_1}{e_1}$$

characteristic of the cured state (assuming here that the thickness variations are small compared to the thickness of the sample).

During crosslinking between T_i and T_f, uncured and cured phases coexisted in the sample. Thus, we considered that the volume expansion coefficient followed an ideal mixture law with an uncured part and a cured part. For a given temperature T,

$$\Delta e_T(T) = \left(\int_{T_i}^{T} (1 - X)k_{uc}\, dT\right) + \left(\int_{T_i}^{T} Xk_c\, dT\right)$$

where k_{uc} is characteristic of the uncured state and k_c is characteristic of the cured state.

Binary and ternary blend did not show any evidence of state change (heat flux curves) during crosslinking, between T_i and T_f. Consequently, for these samples, k_{uc} was determined from the thickness evolution before T_i ($k_{uc} = k_0$) and k_c was determined from the thickness evolution after T_f ($k_c = k_1$). For the different binary and ternary blends, α_0 varied from 6.7 to 7.0×10^{-4} K^{-1} and α_1 varied from 3.7 to 4.7×10^{-4} K^{-1} in good agreement with literature.[20]

For filled samples (TBF, BBF, and BMC), the heat curves showed clearly a critical point where a succession of vitrification/devitrification was encountered. k_{uc} was determined from thickness evolution before T_i ($k_{uc} = k_0$). α_0 was estimated for the various samples and ranges between 2.7 to 4.5×10^{-4} K^{-1}. These values corresponded to expansion coefficient of ternary or binary blend corrected by taking into account the volume proportion contained in the filled sample. Thus, thermal expansions of filled blends were essentially due to organic blends. Before the critical point for $X = X_V$, the cured sample was in rubbery state and the cured thermal coefficient k_c was determined with the second cycle of temperature above glass temperature, either by calculation, knowing the rubbery cured state coefficient of the corre-

TABLE II
$\Delta e/e_0$, $\Delta e_T/e_0$, $\Delta e_{SC}/e_0$ for the Binary Blend (BB) and the Ternary Blends (TB) at Different Pressures

Blend	Pressure (MPa)	$\Delta e/e_0$ (%)	$\Delta e_T/e_0$ (%)	$\Delta e_{SC}/e_0$ (%)	$\Delta e_{SC}/e_0$ (%) for 100% BB
BB	1.6	−1.9	6.9	−8.8	−8.8
	4.8	−2.5	6.6	−9.1	−9.1
	8.0	−2.6	6.3	−8.9	−8.9
TB (5% LPA)	1.6	−1.8	7.2	−9.0	−9.2
	4.8	−2.2	6.9	−9.1	−9.3
	8.0	−2.5	6.2	−8.7	−8.9
TB (15% LPA)	1.6	−1.0	6.9	−7.9	−9.3
	4.8	−1.0	6.7	−7.6	−9.0
	8.0	−1.3	6.5	−7.8	−9.2
TB (25% LPA)	1.6	+0.3	6.5	−6.2	−7.8
	4.8	−0.4	6.5	−6.9	−8.8
	8.0	−0.5	6.5	−7.0	−8.9

sponding binary, or by ternary blend. α_c varied from 2.3 to 3.6 $\times$ 10^{-4} K^{-1}. These two methods were in relatively good agreement. After the critical point, we considered that k_{uc} was unchanged and that k_c corresponded to the observed value after curing (α_c varied from 0.3 to 0.7 $\times$ 10^{-4} K^{-1}) because no slope change was observed.

$e(t)$-Δe_T versus time

The shapes of the curves $e(t)$-Δe_T (i.e., thickness evolution versus time only due to polymerization phenomena) were in agreement with those expected (Fig. 3). First of all, thickness was constant and equal to e_0 until the copolymerization beginning. Then, sample thickness evolved because of resin shrinkage and shrinkage compensation (pores formation). Eventually, when the crosslinking was completed, the thickness remained constant because cured resin thermal expansion was the only phenomenon.

Tables II and III presented the total thickness variation between 40 and 160°C, thermal expansion contribution, and by difference, the thickness variation due to copolymerization for BB and TB and for filled blends, respectively. For the BB and the TB without any fillers, the total thickness variation value ranged from −2.6 to +0.3% (positive value corresponds to expansion and negative value corresponds to shrinkage). This value decreased with increasing pressure for a given LPA concentration and increased with LPA concentration for a given pressure. The TB 25% LPA blend 1.6 MPa presented after heating a volume expansion. Low-pressure and high LPA concentration had positive effects on volume shrinkage control. The contribution of thermal expansion depended on LPA concentration. The dependence on pressure vanished as the LPA concentration increased.

The variation Δe_{SC} versus time involved shrinkage (noted S) and compensation (noted C). Because BB contained no LPA, there was no shrinkage compensation. The shrinkage thickness variation was in this case equal to 9.0%. This value was in good agreement with those observed in the literature.[3,7,8,21] Δe_{SC} was roughly constant when expressed on a total mass BB basis, except for 25% LPA 1.6 MPa. Except for this blend, the main phenomenon during polymerization was shrinkage. Shrinkage compensation, if existing, had a minor effect.

For filled blends, the total thickness variation ranged from −1.8 to +0.5%. This variation also decreased with increasing pressure. TBF and BMC at 1.6 MPa exhibited a volume expansion after curing. Δe_{SC} was always higher than for unfilled blend when expressed on a total BB basis. This comparison clearly indicated that shrinkage compensation in filled blend had to be taken into account.

TABLE III
$\Delta e/e_0$, $\Delta e_T/e_0$, $\Delta e_{SC}/e_0$ for the Filled Binary Blend (BBF), the Filled Ternary Blends (TBF), and BMC at Different Pressures

Blend	Pressure (MPa)	$\Delta e/e_0$ (%)	$(\Delta e_T)/e_0$ (%) (100% TB)	$\Delta e_{SC}/e_0$ (%) (100% BB)
BBF	3.2	−1.8	3.3 (5.7)	−5.1 (−8.8)
TBF	1.6	+0.4	2.8 (6.2)	−2.4 (−6.1)
	8.0	−0.8	2.6 (5.7)	−3.4 (−8.6)
BMC	1.6	+0.5	2.8	−2.3
	8.0	−0.6	2.3	−2.9

$e(t)$-Δe_T versus conversion degree

As shown in Figure 4, e_0 + Δe_T during crosslinking was a sigmoid, as we consider a mixture law for Δe_T evaluation. Its amplitude during reaction was about four times lower than Δe_{SC} and consequently could be considered a minor phenomenon. This observation minimized the effect of all hypotheses on thermal expansion (mixture law and k_{uc} and k_c values).

Examination of $e(t)$-Δe_T versus X allowed us to classify the samples into three groups:

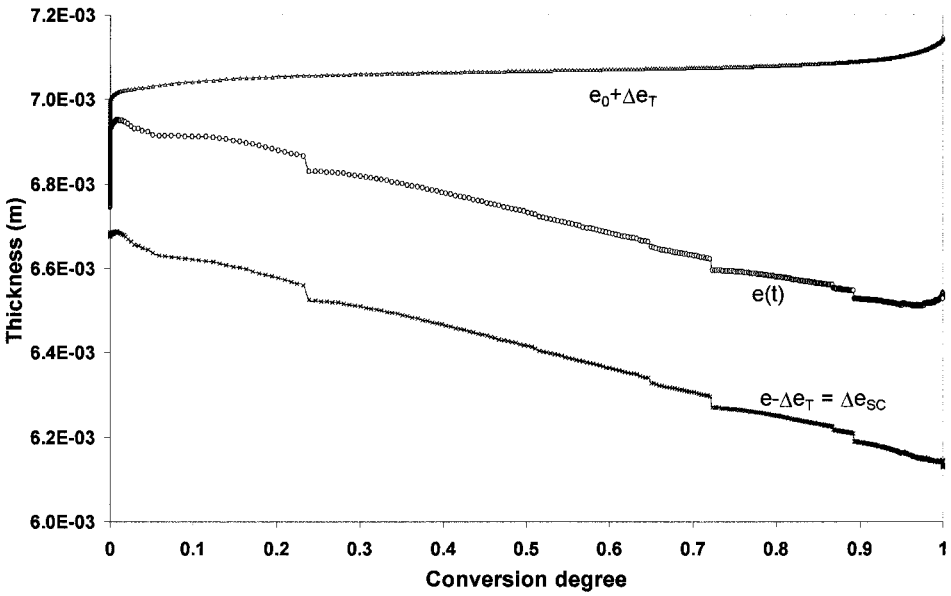

Figure 4 $e(t)$, $e_0 + \Delta e_T$, and $e\text{-}\Delta e_T$ as a function of X for BB at 1.6 MPa.

First group: $e\text{-}\Delta e_T$ was a linear function of X, over the main reaction time (i.e., for $X = X_S$ to $X = 1$) [Fig. 5(a)]. This group contained the binary blend and the ternary blends with 5 wt % of LPA at 1.6, 4.8, and 8.0 MPa, with 15 wt % of LPA at 4.8 and 8.0 MPa and with 25 wt % LPA at 8.0 MPa. X_S conversion degree was always below 0.15.

Second group: $e\text{-}\Delta e_T$ evolved as a linear function from X_S up to X_{CI}. Then, there a transient period which either lasted until $X = 1$ ended quickly and was then followed by an other linear function up to $X = 1$ [in this case, the slopes of two linear parts were not strongly different (Fig. 5(a))]. The ternary blends with 15 wt % LPA at 1.6 MPa and with 25 wt % LPA at 1.6 and 4.8 MPa belong to this group.

Third group: In this case, $e\text{-}\Delta e_T$ as a function of X was a succession of linear parts [Fig. 5(b)]: between $X = 0$ up to X_{CI}, between X_{CF} to X_V, and from X_V to $X = 1$. The slopes were different in the three parts and in the last part the slope was roughly null. Between X_{CI} and X_{CF}, there was a transient part. This group concerned all the filled blends.

Basic steps of thickness evolution

To model the evolution of thickness $e\text{-}\Delta e_T$ ($=\Delta e_{SC}$) during crosslinking, we proposed to decompose the sample evolution into a succession or combination of basic steps. These basic steps are described below. Table IV gives the mathematical expressions of thickness variation and the corresponding rate for each step.

Transient Shrinkage (TS): During this step, the shrinkage started to be established and consequently thickness variation was not a linear function of X.

Steady-State Shrinkage (SSS): Shrinkage was a linear function of X with a slope e_0K_S. Thickness variation rate was proportional to conversion rate. K_S corresponded to the reduction of volume per double-bond opening.

Transient Compensation (TC): Shrinkage induced stresses, which were relaxed by pores formation. In this step, the pores started to be formed. The resulting shrinkage compensation was established; the thickness variation due to this phenomenon was thus not a linear function of X.

Steady-State Compensation (SSC): The shrinkage compensation was established and thickness variation due this phenomenon was a linear function of X with a slope e_0K_C. Its rate was proportional to conversion rate.

Fitting the thickness variation by means of the basics steps

The behavior of all tested blends was described with a combination of the proposed basic steps (Table V). The values of conversion degrees X_S, X_{CI}, and X_V were obtained from experimental analyses for each experiment [see Fig. 5(b) as example] and are reported in Tables VI and VII. The parameters X_{CF}, K_S, K_{SV}, K_C, and K_{CV} were determined by means of an inverse method of parameters estimation. It is based on the minimization of the criterion J by a program using a simplex method

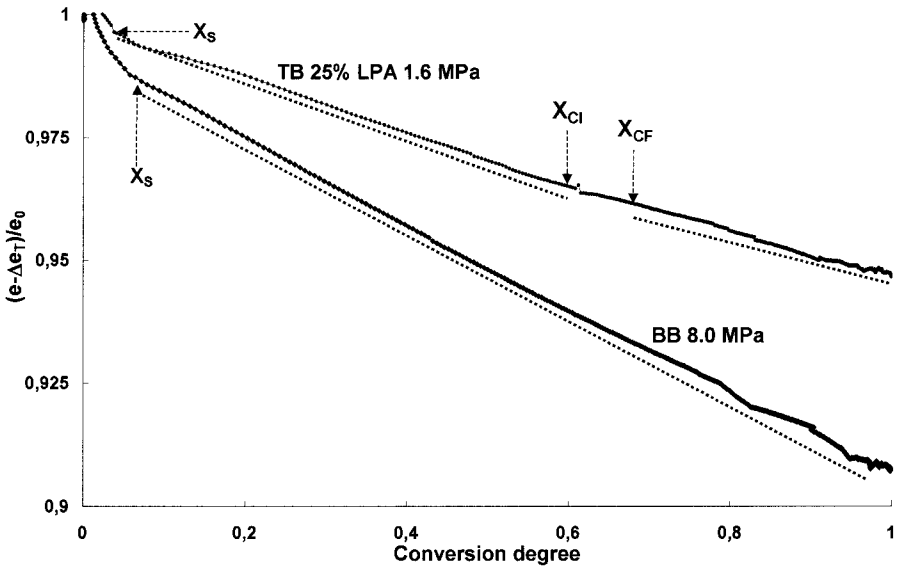

(a)

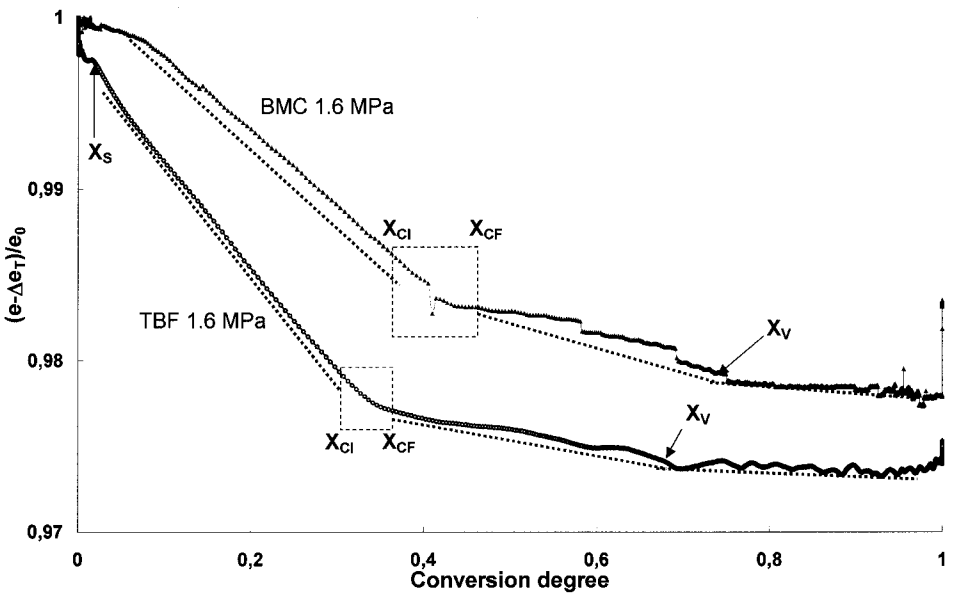

(b)

Figure 5 (a) $(e\text{-}\Delta e_T)/e_0$ as a function of X for BB at 8.0 MPa (group 1) and for TB 25% LPA at 1.6 MPa (group 2). The arrows indicate the important points. (b) $(e\text{-}\Delta e_T)/e_0$ as a function of X for TBF and BMC at 1.6 MPa (group 3). The arrows indicate the important points.

$$J = \sum_{1}^{n} (e_0 + \Delta e_{SC} - (e - \Delta e_T))^2$$

where $e_0 + \Delta e_{SC}$ is the thickness calculated for each experimental value (time step), $e\text{-}\Delta e_T$ is the experimental thickness corrected of thermal expansion effect, and n is the number of experimental values for the experiment.

The theory of inverse method[19] shows that the fitted parameters correspond to an acceptable solution if $\sigma = (j/n)^{1/2}$ is equal to or lower than the error of the experimental value (5 μm). The so calculated thickness evolution curves were compared to the experimental ones without and with taking into account the thermal expansion [see Figs. 6(a–d)]. As clearly seen in these figures, the agreement was excellent. For all the experimental conditions, we verified that σ was lower than 5 μm, proving that for our experimental results, the model was adequate and the set of fitted parameters gave an acceptable solution for all the samples. The optimized parameters K_S, K_C, K_{SV}, and

TABLE IV
Mathematical Expressions of Thickness Variation, Thickness Variation Rate, Parameters, for the Proposed Basic Steps Encountered During Crosslinking

Step	Thickness variation	Thickness variation rate	Parameters
TS transient shrinkage ($X < X_S$)	$\Delta e_S = \int_0^X e_0 K_{TS}\, dX$	$V_S = K_{TS} e_0 dX/dt$	X_S
			K_{TS}
SSS steady-state shrinkage ($X_S < X < X_{CI}$)	$\Delta e_S = K_S e_0 (X - X_S)$	$V_S = K_S e_0 dX/dt$	X_S, X_{CI}
			K_S
TC transient compensation ($X_{CI} < X < X_{CF}$)	$\Delta e_c = \int_{X_{CI}}^X e_0 K\, dX$	$V_C = K e_0 dX/dt$	X_{CI}, X_{CF}
		$K = K_C(1 - F(X))$ $F(X) = \exp[-(AX^4 + B)^2]$	K_C, $F(X)$
SSC steady-state compensation ($X > X_{CF}$)	$\Delta e_C = K_C e_0 (X - X_{CF})$	$V_C = K_C e_0 dX/dt$	X_{CF}
			K_C

K_{CV} values were reported in Tables VI and VII. We applied this methodology to the previously defined three groups.

First group: Before *Xs*, the shrinkage was in a nonsteady state (TS). For $X > Xs$, the shrinkage thickness variation became proportional to X (SSS). As illustrated by Figure 5(a), *Xs* was always lower than 0.15 and, consequently, during the main part of crosslinking, the shrinkage thickness was a linear function of X (slope $e_0 K_S$), indicating that there was no shrinkage compensation. This was an important result because this behavior confirmed the hypothesis generally proposed in the literature, assuming that when no shrinkage compensation occurred, the shrinkage was a linear function of conversion degree.[10,13] All the blends exhibited the same K_S and the same $\Delta e_S/e_0$ when expressed on a total BB basis, suggesting that these parameters were characteristic of the resin. If the LPA contents were too low and the pressure was too high, shrinkage compensation was not observed.

Second group: Before X_{CI} (ranging from 0.6 to 0.9), there was only shrinkage: e-Δe_T followed the evolution described for the first group: TS, SSS. After X_{CI}, shrinkage compensation appeared when the stress developed by shrinkage was too high and was combined to shrinkage. This shrinkage compensation always started via a TC. In some cases, this step existed up to $X = 1$. In the other cases, SSC appeared at a given conversion degree X_{CF}. This shrinkage compensation depends on LPA content and pressure: Low pressure and high LPA content helped shrinkage compensation. The comparison between 25% LPA 1.6 MPa and 25% LPA 4.8 MPa showed that pressure increase delayed the beginning of shrinkage compensation ($X_{CI} = 0.6$ for 25% LPA 1.6 MPa and $X_{CI} = 0.8$ for 25% LPA 4.8 MPa). Decreasing the LPA content had the same effect. For 15% LPA blend at 1.6 MPa, shrinkage compensation appeared very lately ($X_{CI} = 0.9$) and was very intense ($K_C = 9.0$ compared to 2.0 for 25% LPA 1.6 MPa).

Third group [Fig. 6(c–d)]: In this case, the steps were more numerous.

TABLE V
Decomposition of Crosslinking into Basic Steps for the Three Defined Groups

	X_S	X_{CI}	X_{CF}	X_V	
Group 1	(TS; K_{TS}) $e = e_0 + \Delta e_S$		(SSS; K_S) $e = e_0 + \Delta e_S$		
Group 2	(TS; K_{TS}) $e = e_0 + \Delta e_S$	(SSS; K_S) $e = e_0 + \Delta e_S$	(SSS; K_S) + (TC; K_C) $e = e_0 + \Delta e_S + \Delta e_c$	(SSS; K_S) + (SSC; K_C)[a] $e = e_0 + \Delta e_S + \Delta e_c$	
Group 3	$e = e_0 + \Delta e_S$ (SSS; K_S)		$e = e_0 + \Delta e_S + \Delta e_c$ (SSS; K_S) + (TC; K_C)	$e = e_0 + \Delta e_S + \Delta e_c$ (SSS; K_S) + (SSC; K_C)	$e = e_0 + \Delta e_S + \Delta e_c$ (SSS; K_{SV}) + (SSC; K_{CV})

[a] In some cases, this step did not exist.

TABLE VI
Parameter Values for Binary Blend (BB) and Ternary Blends (TB)

Blend	Pressure (MPa)	K_S ($\times 10^{-2}$) (100% BB)	X_S	$X_{CI} - X_{CF}$	K_C ($\times 10^{-2}$) (100% BB)	σ (m) $\times 10^6$	$(\Delta e_S)/e_0$ (%) (100% BB)	$(\Delta e_C)/e_0$ (%) (100% BB)
BB	1.6	−8.2	0.12			4.4	−8.8	
	4.8	−8.3	0.12			2.7	−9.1	
	8.0	−10.0	0.14			2.7	−8.9	
TB	1.6	−9.25 (−9.6)	0.14			2.2	−9.0 (−9.2)	
(5% LPA)	4.8	−8.6 (−9.0)	0.14			3.7	−9.1 (−9.3)	
	8.0	−8.3 (−8.6)	0.14			6.7	−8.7 (−8.9)	
TB	1.6	−9.3 (−10.6)	0.14	0.9–1	9.0 (10.3)	1.6	−8.5 (−9.7)	+0.6 (4.7)
(15% LPA)	4.8	−8.7 (−10.0)	0.12			1.1	−7.6 (−9.0)	
	8.0	−7.4 (−8.5)	0.14			4.4	−7.8 (−9.2)	
TB	1.6	−6.2 (−8.0)	0.14	0.6–0.7	2.0 (2.5)	1.3	−6.9 (−8.8)	+0.7 (3.2)
(25% LPA)	4.8	−7.0 (−8.9)	0.14	0.8–1	2.6 (3.3)	1.6	−7.2 (−9.2)	+0.3 (1.4)
	8.0	−6.8 (−8.6)	0.20			3.8	−7.0 (−8.9)	

First, shrinkage was only observed. e-Δe_T was a linear function of X up to X_{CI} (SSS). K_S was found to be approximately 1.5 times higher than for binary or ternary blends.

Between X_{CI} and X_{CF}, a transient state of shrinkage compensation superimposed on SSS. Starting from X_{CF}, the shrinkage compensation exhibited a steady state where e-Δe_T became again a linear function of X (SSS+SSC). The shrinkage compensation started for conversion degree much lower than for ternary blends (X_{CI} varied from 0.25 to 0.55 for the filled blend). Moreover, K_C and $(\Delta e_C/e_0)$ were higher than for ternary blends. BBF also presented shrinkage compensation, although there was no LPA. Shrinkage compensation in the ternary-filled blends combined LPA and fillers effects. The presence of fillers or fibers created an additional interface with the organic blend. A part of stress due to shrinkage was relaxed in this zone to low mechanical resistance.[22,23] The pressure effect was the same as for ternary blends: increasing pressure delayed the beginning of pores formation[24] and increased duration (X_{CF}-X_{CI}) of the setting of shrinkage compensation. Pressure also decreased shrinkage compensation amplitude [K_C and $(\Delta e_C/e_0)$]. The applied pressure was opposed to porosity formation.

After the critical point X_V, the system evolved via a succession of vitrification/devitrification. Shrinkage (characterized by e_0K_{SV}) and shrinkage compensation (characterized by e_0K_{CV}) were superposed, giving a new linear part with a lower slope. From X_V, the macromolecular mobility of the chains was reduced and the reaction was spread out in time. The obtained values of K_{SV} and K_{CV} were lower than the values of K_S and K_C.

CONCLUSION

A very efficient apparatus already used to study high viscous reactive blends was extended to liquid systems (unfilled mixtures). During dynamical heating, the basic steps inducing volume change were identified as thermal expansion, shrinkage, and shrinkage compensation. For filled blends, an additional step (vitrification/devitrification) was also pointed out. All these basic steps were modeled and quantified. After subtraction of the contribution of thermal expansion, thickness variation due to shrinkage was shown to be a linear function of the conversion degree. Moreover, thickness variation due to shrinkage compensation was also a linear function of conversion degree. The proposed model was general and could fit binary or ternary blends as well as more complex blends with fillers and fibers. The results of this model could be used reversibly to evaluate the pressure variation during the curing of a sample in a mold.

TABLE VII
Parameter Values for Charged Binary Blend (BBF), Ternary Blend (TBF), and BMC

Blend	Pressure (MPa)	K_S ($\times 10^{-2}$) (100% BB)	$X_{CI} - X_{CF}$	K_C ($\times 10^{-2}$) (100% BB)	X_V	K_{SV} ($\times 10^{-2}$) (100% BB)	K_{CV} ($\times 10^{-2}$)	σ (m) ($\times 10^6$)	$(\Delta e_S)/e_0$ (%) (100% BB)	$(\Delta e_C)/e_0$ (%) (100% BB)
BBF	3.2	−6.9 (−11.9)	0.55–0.64	2.5 (4.3)	0.84	−4.4 (−7.6)	1.1	3.1	−6.0 (−10.3)	+0.9 (1.5)
TBF	1.6	−7.1 (−17.9)	0.27–0.37	6.1 (15.4)	0.70	−4.6 (−11.6)	3.8	4.0	−6.0 (−15.1)	+3.6 (9.1)
	8.0	−5.5 (−13.9)	0.35–0.68	5.0 (12.6)	0.70	−1.3 (−3.3)	0.3	2.9	−4.3 (−10.8)	+0.9 (2.3)
BMC	1.6	−4.2 (−15.5)	0.35–0.50	2.8 (28.6)	0.74	−2.8 (−10.5)	2.0	1.5	−3.7 (−13.7)	+1.4 (5.2)
	8.0	−4.3 (−15.9)	0.55–0.78	4.0 (40.8)	0.70	−3.2 (−11.8)	1.9	2.1	−3.6 (−13.3)	+0.7 (2.9)

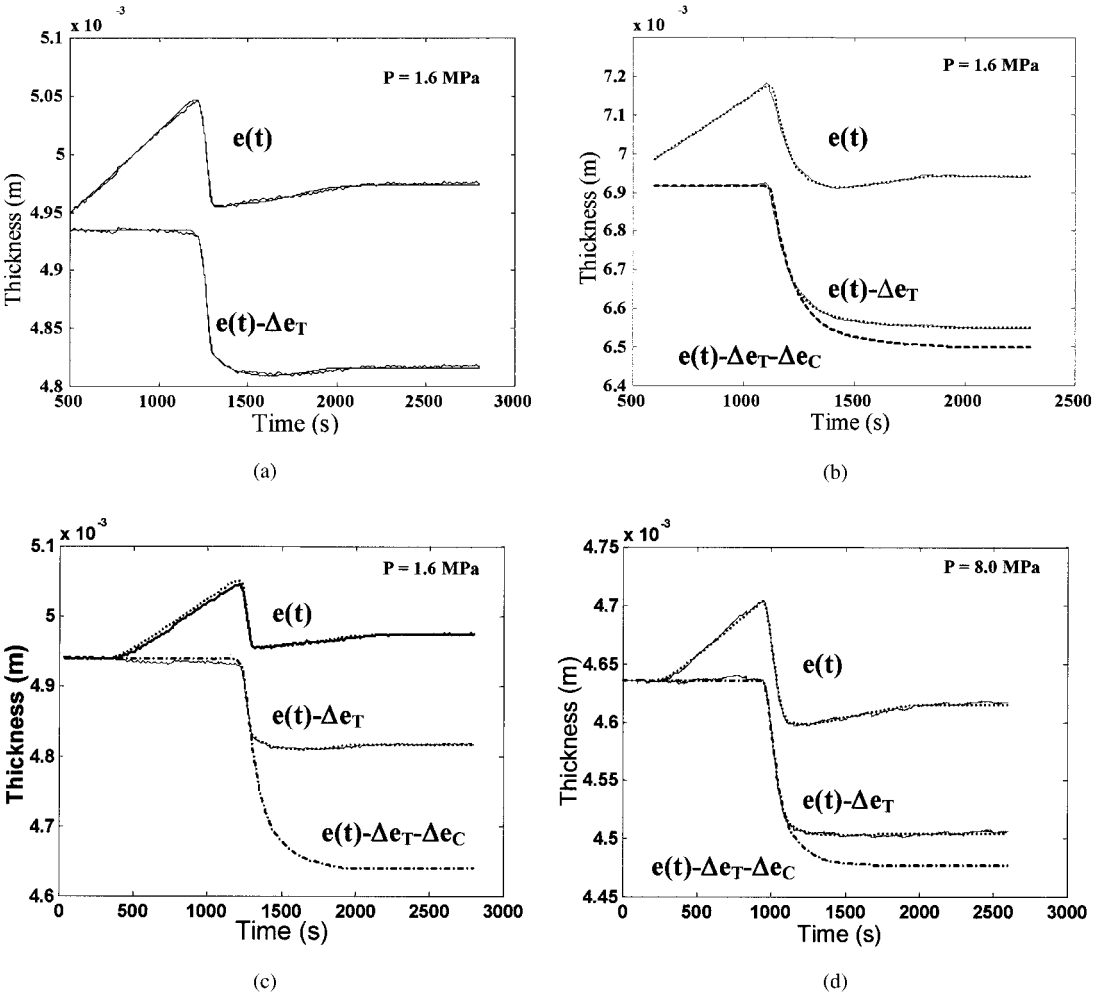

Figure 6 (a) Comparison between experimental curve (solid line) and modeled (dashed line) curve for $e(t)$ and $e(t)$-Δe_T as a function of time (t) for BB at 1.6 MPa. (b) Same as (a) for TB 25% LPA at 1.6 MPa. (c) Same as (a) for TBF at 1.6 MPa. (d) Same as (a) for BMC 8.0 MPa.

Important results on the neat resin behavior were obtained. The hypothesis of linear dependence of shrinkage to conversion degree was verified. Fundamental constants were identified: shrinkage amplitude (-9%) and kinetic parameter (K_S). By testing ternary blend with various LPA contents at various molding pressures, we observed that a LPA content higher than 15% with a low pressure allowed shrinkage compensation. Increasing pressure had multiple effects: limited thermal expansion and shrinkage compensation, and a delayed shrinkage beginning. The model for filled blends took into account state transition. Comparison between binary and ternary blend and filled blends highlighted the benefic effect of fillers and fibers on shrinkage compensation, even without any LPA. The mechanism of shrinkage compensation by fillers or fibers and the combination of LPA and fillers remained to be determined more precisely.

During thermoset processing, a cooling down and pressure release period succeeded to the heating period, which is not taken into account in this work. This has to be considered to have a global appreciation of the behavior of such system from a practical point of view and will be the subject of further work.

The authors acknowledge A. Millisher for his Ph.D. thesis and N. Lefèvre for help to mold conception, Ph. Grandet for experiments, M.-L. Guegan and J.-P. Ollivier for fruitful discussions, and Menzolit and the region "CENTRE" for financial support.

References

1. Serré, Ch.; Vayer, M.; Erre, R.; Boyard, N.; Ollive, C. J Mater Sci 2001, 36, 113.
2. Li, W.; Lee, L. J Polym 1998, 39, 5677.
3. Li, W.; Lee, L. J Polym 2000, 41, 685.
4. Atkins, K. E.; Koleske, J V.; Smith, P. L.; Walter, E. R.; Mattews, V. E. in Proceedings of the 31st Annual Technical Conference of the Society of Plastics Industry; 1976.
5. Atkins, K. E. Polymer Blends; Paul, D. R.; Newman, S., Eds.; Academic Press: New York, 1978; Chapter 23.

6. Atkins, K. E. Low profile additive: shrinkage control mechanism and applications. in Sheet Molding Compound Materials: Science and Technology; Hanser, H. K., Ed.; 1993.
7. Kinkelaar, M.; Lee, L. J. J Appl Polym Sci 1992, 45, 37.
8. Kinkelaar, M.; Wang, B.; Lee, L. J Polym 1994, 35, 3011.
9. Van Assche, G.; Van Hemelrijck, A.; Rahier, H.; Van Mele, B. Thermochim Acta 1996, 286, 209.
10. Hill, R. R.; Muzumdar, S. V.; Lee, L. J Polym Eng Sci 1995, 35, 852.
11. Millischer, A.; Delaunay, D.; Jarny, Y. in Proceedings Cancom 2001; Third Canadian International Composite Conference, 21–24 August 2001, Montreal.
12. Millischer, A. Ph.D. Thesis, Université de Nantes, 2000.
13. Boyard, N.; Vayer, M.; Sinturel, C.; Erre, R.; Delaunay, D. J Appl Polym Sci 2003, 88, 1258.
14. Odian, G. Principles of Polymerization, 3rd ed.; Wiley: New York, 1991; Chapter 3.
15. Martin, J. L.; Cadenato, A.; Salla, J. M. Therm Acta 1997, 306, 115.
16. Pascault, J.-P.; Sautereau, H.; Verdu, J.; Williams, R. J. J. Thermosetting Polymers; Hudgin, D. E., Ed.; Marcel Dekker: New York, 2002; Chapter 5.
17. Kubota, H. J Appl Polym Sci 1975, 19, 2279.
18. Lucas, J. C.; Borrajo, J.; Williams, R. J. J Polym 1993, 34, 1886.
19. Beck, J. V.; Blackwell, B.; St. Clair, C. Inverse Heat Conduction; Wiley-Interscience: New York, 1985.
20. Verdu, J. Composites 1997, 37, 80.
21. Huang, Y.-J.; Liang, C-M. Polymer 1996, 37, 401.
22. Bucknall, C. B.; Partridge, I. K.; Phillips, M. J Polym 1991, 32, 636.
23. Chan-Park, M. B.; McGarry, F. J. J Adv Mater 1995, 27, 47.
24. Zhang, Z.; Zhu, S. Polymer 2000, 41, 3861.